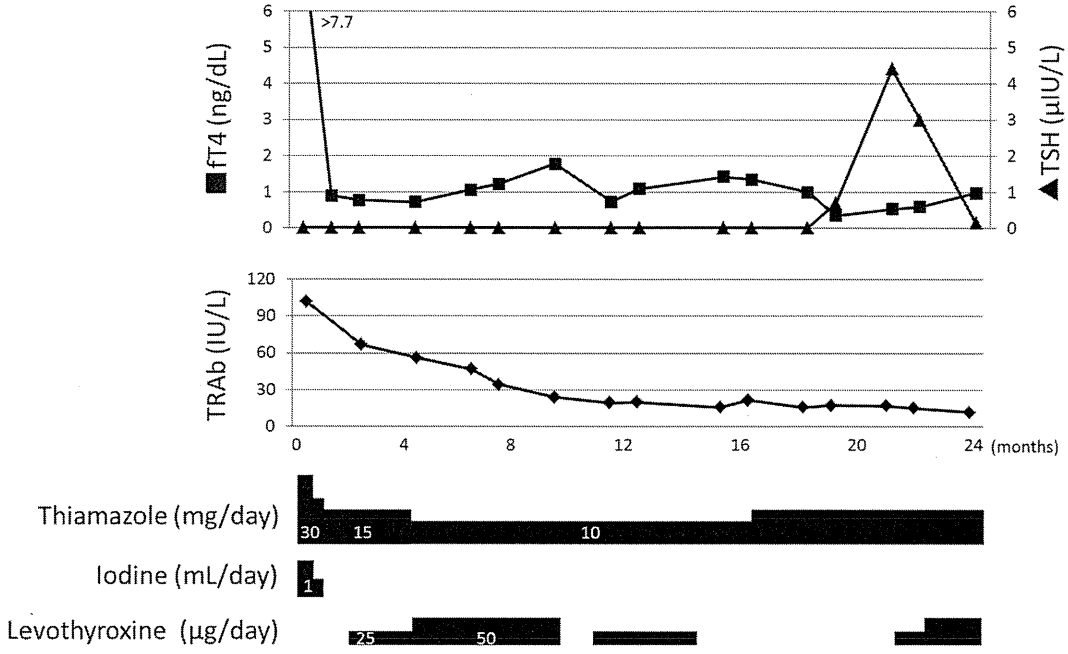

Fig. 4. Clinical course of the proband (III-4). Free thyroxine (fT4) was normalized within a month. Thyroid-stimulating hormone (TSH) levels had been suppressed. Anti-thyroid stimulating hormone receptor antibody (TRAb) titers were reduced.

was not performed.

She was referred to the pediatric endocrinology division at 10 yr of age because of weight loss. On examination, hand tremor and tachycardia (139 bpm) were apparent. Her thyroid was soft and large by palpation. She also had exophthalmos. Blood tests revealed marked hyperthyroidism with a suppressed thyroid-stimulating hormone level (<0.01 μIU/L, reference 0.5–5) and elevated free triiodothyronine (>32.55 pg/mL, reference 2.3–4.0) and free thyroxine levels (>7.77 ng/dL, reference 0.90–1.70). Ultrasonography revealed an enlarged thyroid (estimated size, >34.4 mL, reference 2.9–6.3 (5, 6)), which had heterogeneously low echogenicity. Marked hypervascularity was shown by color Doppler imaging (Fig. 3). The diagnosis of Graves' disease was confirmed by elevated anti-thyroid stimulating hormone receptor antibody (102 IU/L, reference <1.0). Treatment with 30 mg of thiamazole and 1 mL of 2.5% aqueous iodine solution improved clinical symptoms within a month. Then, her anti-thyroid stimulating hormone receptor antibody titers were found to be reduced. Her serum thyroid-stimulating hormone levels had been suppressed. She needed 15 mg of thiamazole two years after diagnosis (Fig. 4).

She has suffered from bronchial asthma with a high immunoglobulin E (IgE) level (511 IU/mL, reference <173) for five years. Her bronchial asthma has been well controlled with montelukast and inhaled beclomethasone. Other immunological tests, including serum levels of immunoglobulins (IgG, IgA, IgM) and blastoid transformation of lymphocytes in response to concanavalin-A and phytohemagglutinin, were within normal limits.

II-3

The proband's uncle is 43 yr old. A periodic medical examination at school revealed proteinuria at 10 yr of age. He presented with enuresis until 11 yr of age. The results of renal

biopsy at 14 yr of age and information about medical treatment was not available. His renal function continued to deteriorate. At 18 yr of age, he was placed on chronic hemodialysis. At 19 yr of age, he had a kidney transplant from his elder brother (II-2). He had complained visual impairment since his late thirties. At 40 yr of age, an ocular fundus examination revealed macular degeneration of his left eye and bilateral optic nerve dysplasia (Fig. 2C, D). At 42 yr of age, retinal detachment of his left eye occurred.

II-4

The proband's mother is 37 yr old. She presented with enuresis until 12 yr old. At 12 yr of age, a periodic medical examination at school revealed proteinuria for the first time. Ultrasonography revealed bilateral renal hypoplasia. At 14 yr of age, left renal biopsy revealed no specific findings. At 26 yr of age, she became pregnant with the proband (III-4), and her renal function became worse. Repeated renal biopsy revealed no specific findings (Fig. 2E). When she became pregnant with a fetus (III-6) at 32 yr of age, her renal function further deteriorated and hypertension developed. The family elected to interrupt the pregnancy at 10 wk of gestation. She was obese, and her body mass index was 32.8 at her last visit.

Mutation analysis of the *PAX2* gene

After obtaining written informed consent, we extracted genomic DNA from peripheral blood samples or nails of four family members (II-3, II-4, III-4 and III-7) using standard protocols. Genomic DNA samples were PCR-amplified for the coding 11 exons and their splice sites of the *PAX2* gene (7), and the PCR products were subjected to direct sequencing from both directions on an autosequencer. All of them had a heterozygous mutation (c.76dupG, p.Val26Glyfs*28) that inserts an extra guanine nucleotide in a stretch of seven guanine nucleotides (Fig. 1B).

Discussion

We described a Japanese family with renal coloboma syndrome and a heterozygous mutation (c.76dupG, p.Val26Glyfs*28) in exon 2 of the *PAX2* gene. Clinical manifestations varied within the family. Ocular fundus manifestations included normal fundus, optic nerve dysplasia, and retinal detachment. Renal manifestations included renal hypoplasia, urinary concentrating defects, proteinuria and end-stage renal insufficiency. One of the two patients with renal failure had a kidney transplant.

The c.76dupG mutation is one of the most frequent *PAX2* mutations (8). It is predicted to have a premature termination codon located in 54–56 nucleotides upstream of the subsequent exon-intron junction. The c.76dupG mutation may trigger nonsense-mediated decay (NMD), although whether the mutation triggers NMD remains to be clarified. Even if the mutant RNA is not destroyed by NMD, the c.76dupG mutation would lead to a truncated protein lacking any functional domains. Clinical presentation of the c.76dupG carriers is known to be highly variable between individuals and even within a family (3, 7). Genotype-phenotype correlation is not evident among *PAX2* mutation carriers. It has been hypothesized that genetic, epigenetic or environmental factors may modulate the clinical manifestations in humans and mice with *PAX2* mutations (9, 10).

Interestingly, the proband had an atypical complication, Graves' disease. Graves' disease is an autoimmune disorder mediated by agonistic antibodies to the thyroid stimulating hormone receptor, which is the commonest cause of hyperthyroidism in childhood and adolescence. *PAX2* mutations or renal coloboma syndrome associated with Graves' disease has not been reported so far. One previous study showed that the increased risk of Henoch-Schönlein purpura nephritis, a putative immune-mediated glomerular disease, was associated with *PAX2* gene polymorphisms (11). Although coexistence

of renal coloboma syndrome and Graves' disease in the proband could be only coincidental, we think it probable that *PAX2* mutations may be associated with development of Graves' disease. PAX2 has been known to be expressed in a subset of lymphocytes (12), and thus would have a physiological role in the immune system. PAX2 represses human ß-defensin 1 expression through binding to the promoter (13). Functional single nucleotide polymorphisms of ß-defensin 1 were reported to be risk factors for development of systemic lupus erythematosus (14) and autoimmune thyroid diseases in type 1 diabetes patients (15). We speculate that *PAX2* mutations may increase the risk of autoimmune diseases, including Graves' disease, through alterations of human ß-defensin 1 expression.

In summary, we reported a patient with a familial *PAX2* mutation, who also had Graves' disease. Further study will clarify whether *PAX2* mutations can be a risk factor for development of autoimmune diseases.

Acknowledgements

We thank the family for participating in this study. We also thank Ms. Reiko Iwano for technical assistance, Drs. Hidekazu Moriya, Eiji Hiwatari and Kazunari Yoshida for providing us with clinical information and Dr. Satoshi Narumi for fruitful discussion and critical reading of the manuscript.

References

1. Rieger G. Zum Krankheitsbild der Handmannschen Sehnerven-anomalie: 'Winderblum'-('Morning Glory') syndrom? Klin Monatsbl Augenheilkd 1977;170: 697–706. [Medline]
2. Bower M, Salomon R, Allanson J, Antignac C, Benedicenti F, Benetti E, *et al.* Update of PAX2 mutations in renal coloboma syndrome and establishment of a locus-specific database. Hum Mutat 2012;33: 457–66. [Medline]
3. Ford B, Rupps R, Lirenman D, Van Allen MI, Farquharson D, Lyons C, *et al.* Renal-coloboma syndrome: prenatal detection and clinical spectrum in a large family. Am J Med Genet 2001;99: 137–41. [Medline]
4. Eccles MR, Schimmenti LA. Renal-coloboma syndrome: a multi-system developmental disorder caused by PAX2 mutations. Clin Genet 1999;56: 1–9. [Medline]
5. Ueda D. Normal volume of the thyroid gland in children. J Clin Ultrasound 1990;18: 455–62. [Medline]
6. Chanoine JP, Toppet V, Lagasse R, Spehl M, Delange F. Determination of thyroid volume by ultrasound from the neonatal period to late adolescence. Eur J Pediatr 1991;150: 395–9. [Medline]
7. Schimmenti LA, Cunliffe HE, McNoe LA, Ward TA, French MC, Shim HH, *et al.* Further delineation of renal-coloboma syndrome in patients with extreme variability of phenotype and identical PAX2 mutations. Am J Hum Genet 1997;60: 869–78. [Medline]
8. Amiel J, Audollent S, Joly D, Dureau P, Salomon R, Tellier AL, *et al.* PAX2 mutations in renal-coloboma syndrome: mutational hotspot and germline mosaicism. Eur J Hum Genet 2000;8: 820–6. [Medline]
9. Cross SH, McKie L, West K, Coghill EL, Favor J, Bhattacharya S, *et al.* The Opdc missense mutation of Pax2 has a milder than loss-of-function phenotype. Hum Mol Genet 2011;20: 223–34. [Medline]
10. Iatropoulos P, Daina E, Mele C, Maranta R, Remuzzi G, Noris M. Discordant phenotype in monozygotic twins with renal coloboma syndrome and a PAX2 mutation. Pediatr Nephrol 2012;27: 1989–93. [Medline]
11. Yi ZW, Fang XL, Wu XC, He XJ, He QN, Dang XQ, *et al.* Role of PAX2 gene polymorphisms in Henoch-Schönlein purpura nephritis. Nephrology 2006;11: 42–8. [Medline]
12. Zhai QJ, Ozcan A, Hamilton C, Shen SS, Coffey D, Krishnan B, *et al.* PAX-2 expression in non-neoplastic, primary neoplastic, and metastatic neoplastic tissue: A comprehensive immunohistochemical study. Appl Immunohistochem Mol Morphol 2010;18:

323–32. [Medline]
13. Bose SK, Gibson W, Bullard RS, Donald CD. PAX2 oncogene negatively regulates the expression of the host defense peptide human beta defensin-1 in prostate cancer. Mol Immunol 2009;46: 1140–8. [Medline]
14. Sandrin-Garcia P, Brandão LA, Guimarães RL, Pancoto JA, Donadi EA, Lima-Filho JL, *et al.* Functional single-nucleotide polymorphisms in the DEFB1 gene are associated with systemic lupus erythematosus in Southern Brazilians. Lupus 2012;21: 625–31. [Medline]
15. Guimarães RL, Segat L, Rocha CR, Brandão LA, Zanin V, Araujo J, *et al.* Functional polymorphisms of DEFB1 gene in type 1 diabetes Brazilian children. Autoimmunity 2009;42: 406–13. [Medline]

Growth Hormone & IGF Research 23 (2013) 89–97

Contents lists available at SciVerse ScienceDirect

Growth Hormone & IGF Research

journal homepage: www.elsevier.com/locate/ghir

Novel compound heterozygous mutations of the growth hormone-releasing hormone receptor gene in a case of isolated growth hormone deficiency

Akiko Soneda [a], Masanori Adachi [a,*], Koji Muroya [a], Yumi Asakura [a], Masaki Takagi [b], Tomonobu Hasegawa [b], Hiroshi Inoue [c], Mitsuo Itakura [c]

[a] Department of Endocrinology and Metabolism, Kanagawa Children's Medical Center, Japan
[b] Department of Pediatrics, Keio University School of Medicine, Japan
[c] Division of Genetic Information, Institute for Genome Research, The University of Tokushima, Japan

ARTICLE INFO

Article history:
Received 12 September 2012
Received in revised form 27 February 2013
Accepted 13 March 2013
Available online 18 April 2013

Keywords:
Isolated growth hormone deficiency
Pituitary hypoplasia
Growth hormone-releasing hormone receptor
Short stature
Splice donor site

ABSTRACT

Objective: To elucidate the pathogenesis of isolated growth hormone (GH) deficiency in a Japanese girl without consanguinity.
Design: A 2-year-old girl of height 77.2 cm (−3.0 SD for Japanese girls) was found to have an insulin-like growth factor (IGF)-1 level of 7 ng/mL and IGF binding protein-3 (IGFBP-3) level of 0.41 μg/mL. GH responded modestly to a series of pharmacological stimulants, increasing to 2.81 ng/mL with insulin-induced hypoglycemia, 3.78 ng/mL with arginine, and 3.93 with GH-releasing hormone (GHRH). Following direct sequencing of the GHRH receptor (*GHRHR*) gene, evaluation by the luciferase reporter assay, immunofluorescence study, and in vitro splicing assay with minigene constructs was conducted.
Results: Novel compound heterozygous *GHRHR* gene mutations were identified in the patient. A p.G136V substitution elicited no luciferase activity increment in response to GHRH stimulation, with normal membranous expression. Splicing assay demonstrated that the IVS2 + 3a > g mutation would lead to aberrant splicing.
Conclusions: A case of isolated GH deficiency due to novel *GHRHR* gene mutations was identified.

1. Introduction

Growth hormone (GH) deficiency (GHD) refers to inadequate GH secretion from the anterior pituitary gland. When GHD occurs in combination with other pituitary hormone deficiencies, it is defined as multiple pituitary hormone deficiency; when GHD presents without other pituitary involvement, it is called isolated GHD (IGHD). The reported incidence of IGHD has varied widely between 1 in 3500 and 1 in 10,000 live births [1–5]. This great variation may be partly due to the different cut-off thresholds for defining IGHD when interpreting pharmacological stimulation tests for GH.

Although IGHD is usually idiopathic, 5–30% of IGHD patients have genetic backgrounds, including mutations involving the *GH1* gene and GH-releasing hormone receptor (*GHRHR*) gene. Of these, *GHRHR* gene mutations are extremely rare, with most cases described in consanguineous families [6–17]. Genetic screening for IGHD patients in the UK [8] and Netherlands [18] failed to identify any sporadic cases with *GHRHR* mutation. Furthermore, a Japanese study examining the effects of *GHRHR* mutations in 127 short children revealed 1 IGHD family with a homozygous mutation [19]. We herein report the case of a Japanese girl found to have IGHD due to novel heterozygous *GHRHR* gene mutations.

2. Patient report

A 2-year-old Japanese girl was referred for the evaluation of short stature (Fig. 1a). Her non-consanguineous parents were in good health. Her father was 169.5 cm tall (−0.2 SD for Japanese men according to the national reference data [20] and her mother 156.3 cm tall (−0.3 SD for Japanese women). Her 4-year-old brother showed normal growth and development (Fig. 1b). The patient was born at term following a normal pregnancy and uncomplicated vaginal delivery in cephalic presentation. Her birth weight was 3236 g (+0.6 SD) and height 50.0 cm (+0.8 SD). There were no episodes suggestive of hypoglycemia. As depicted in Fig. 1a, her growth curve was quite worrisome throughout her infancy. When she presented at the hospital, her height was 77.2 cm (−3.0 SD), weight 8.9 kg (body mass index: −0.4 SD [20]), and head circumference 44.0 cm (−2.1 SD). Mild frontal bossing was observed. Her developmental milestones were appropriate for her age. According to the Greulich and Pyle method, bone age was 1 year and 8 months. Laboratory findings showed normal results, including the complete blood count, serum electrolytes, and liver and renal function tests. Thyroid function was also normal: TSH, 3.73 μIU/mL (reference range 0.50–5.00); free T4, 1.16 ng/dL [14.9 pmol/L] (reference range 0.90–1.70 ng/dL); and

* Corresponding author at: Department of Endocrinology and Metabolism, Kanagawa Children's Medical Center, Mutsukawa 2-138-4, Minami-ku, Yokohama 232-8555, Japan. Tel.: +81 45 711 2351; fax: +81 45 742 7821.
E-mail address: madachi@mars.sannet.ne.jp (M. Adachi).

1096-6374/$ – see front matter © 2013 Elsevier Ltd. All rights reserved.
http://dx.doi.org/10.1016/j.ghir.2013.03.003

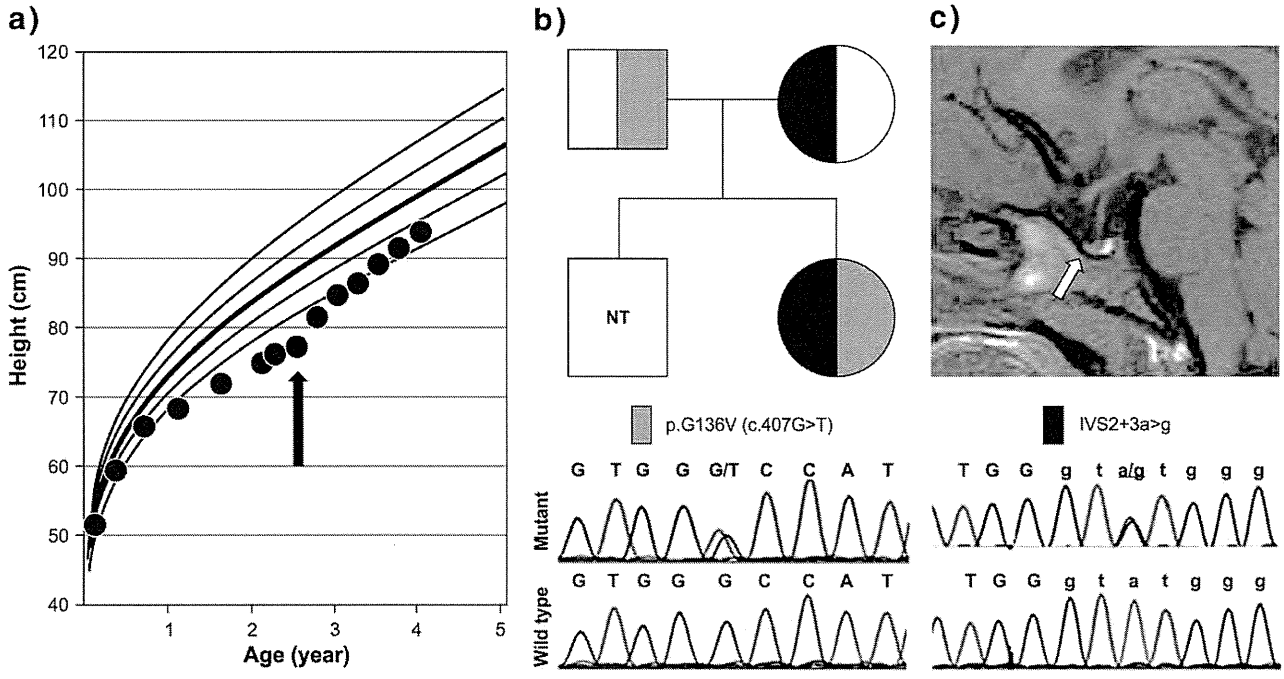

Fig. 1. Clinical characteristics of the patient. a) Height curves. The introduction of GH treatment is depicted by an arrow. b) Family tree. The gray symbol denotes G136V mutation in the *GHRHR* gene, whereas the black symbol indicates IVS2 + 3a > g mutation. Electropherogram of each mutation is shown under the family tree. NT: not tested. c) MR image taken at age 2 years 3 months. The arrow indicates the pituitary gland.

free T3, 3.75 pg/mL [5.76 pmol/L] (reference range 2.30–4.30 pg/mL). Gonadotropins (FSH, 5.11 IU/L; LH, 0.10 IU/L) as well as PRL (23.3 ng/mL) were also appropriate for the patient's age. Because of low levels of both IGF-1 (7 ng/mL; reference range for female infants, 37–229 ng/mL) and IGFBP-3 (0.41 μg/mL; reference range for female infants, 1.33–2.19 μg/mL), a series of GH stimulation tests was conducted. An MRI of the sellar region revealed a pituitary gland of normal size and shape (Fig. 1c). At the age of 2.5 years, GH treatment was initiated at the dose of 0.20 mg/kg/week, divided into 6 injections per week. The patient showed an excellent response to this treatment (Fig. 1a).

3. Materials and methods

3.1. Hormonal evaluations

Serum GH level was determined by a specific RIA kit (GH KIT Daiichi®; TFB Inc., Tokyo, Japan) with recombinant GH (WHO 98/574) set as the standard [21]. IGF-1 concentration was measured by IRMA (IGF-1 IRMA Daiichi®; TFB INC.), and IGFBP-3 concentration was measured by RIA (IGFBP-3 COSMIC®; Cosmic Corporation, Tokyo, Japan). GH stimulation tests were carried out in an overnight fasting state using 4 pharmacological stimuli: insulin-induced hypoglycemia (0.1 U/kg weight); arginine (0.5 g/kg); GHRP-2 (GHRP KAKEN 100®; Kaken Pharmaceutical Co. Ltd., Tokyo, Japan, 2 μg/kg); and GHRH (GRF Sumitomo®, Dainippon Sumitomo Pharma Co. Ltd, Osaka, Japan, 1 μg/kg). GHRP-2 is a ghrelin receptor ligand, more likely acting through the enhancement of hypothalamic GHRH release [22,23].

3.2. Mutation detection

Genomic DNA was extracted from peripheral blood leukocytes using standard techniques. The entire coding sequence of *GH-1* comprising 7 exons and of the *GHRHR* gene comprising 13 exons, including intron–exon boundaries and promoter regions, were amplified by PCR and then directly sequenced by the BigDye Terminator v3.1 Cycle Sequencing Kit on an ABI Prism 310 genetic analyzer (Applied Biosystems, Foster City, CA). PCR primers and conditions for analysis of the *GHRHR* gene were according to those reported in a previous study [6]. In addition, the Multiplex Ligation-dependent Probe Amplification assay (MLPA) was performed using the MLPA kit for GHD (Salsa® MLPA® kit for GHD; MRC-Holland, Amsterdam, Netherlands), which can analyze the following genes involved in genetic GHD: *GH1*, *GHRHR*, *PIT1*, *PROP1*, *LHX3*, *LHX4*, and *HESX1*.

3.3. Construction of expression vectors and site-directed mutagenesis

The wild-type (WT)-GHRHR expression vector was constructed by generating cDNA encoding human *GHRHR* gene by PCR from human pituitary cDNA (Gene Pool Human cDNA; Invitrogen, Carlsbad, CA) and then cloning it into pEGFP-N1 (Clontech Laboratories Inc., Palo Alto, CA) via the introduced *Hin*dIII/*Bam*HI restriction sites.

The p.G136V substitution was introduced by site-directed mutagenesis using the primer set comprising GHRHR-Ex5-Up_ (5′-ACACC GTGGTCCATAGCATCTCTATTGTAG-3′) and GHRHR-Ex5-Lo_(5′-TGCT ATGGACCACGGTGTAGATAATG-3′ (mutated nucleotide underlined). The resulting purified amplicons were digested and then subcloned into the *Hin*dIII/*Bam*HI site of pEGFP-N1. The 3′ end of the vector contained a GFP sequence, thus yielding the following constructs: GFP-GHRHR-Ex5-WT or -mutant. Mutagenesis was confirmed by direct DNA sequencing.

3.4. Cell culture and GHRH-induced luciferase reporter assay

Human embryonic kidney (HEK) 293 cells were maintained in DMEM supplemented with 1% penicillin (10,000 U/mL), streptomycin (10,000 μg/mL), and 10% fetal bovine serum (FBS). Activation of G protein-coupled signal transduction by GHRH (WT or mutant) was studied using luciferase assays. Gs-coupled signaling was analyzed with a reporter vector containing the cAMP response element (CRE-luc; pGL4.29, Promega, Fitchburg, WI). We seeded HEK-293

cells in a 12-well plate and transfected the cells with 400 ng of each GHRHR construct (empty vector or WT or p.G136V) along with 800 ng of CRE-luc reporter vector and 2 ng pRL-CMV internal control vector (Promega) using Lipofectamine 2000. Twenty-four hours after transfection, the medium was removed, and the cells were incubated with 0 or 10^{-8} mol GHRH molecules at 37 °C. Cells were harvested and analyzed sequentially for firefly and Renilla luciferase activities (Dual-Luciferase Reporter Assay System, Promega) according to the manufacturer's protocol. Experiments were conducted in quadruple and repeated at least 3 times.

3.5. Immunofluorescence study

We created an N-terminal hemagglutinin (HA)-tagged GHRHR (HA-GHRHR) expression vector by inserting the HA sequence (TACCCATACGATGTTCCAGATTACGCT) between c.66C and c.67C of the *GHRHR* gene. G136V was introduced by site-directed mutagenesis. HeLa cells grown on sterile glass coverslips were co-transfected with each HA-GHRHR construct (WT or G136V) and a membrane-targeting vector (fusion construct of membrane targeting signal and enhanced red fluorescent protein). Transfected cells were fixed for 10 min in 4% paraformaldehyde/PBS and were incubated with 1:200 anti-HA Alexa Fluor® 488 conjugate antibody (clone 16B12, Invitrogen) at room temperature for 60 min. The fixed cells were permeabilized for 10 min in 0.1% Triton X-100/PBS for staining intracellular antigens. The coverslips were mounted with Vectashield Mounting Medium (Vector Laboratories, Burlingame, CA), and were observed under a confocal microscope (Leica TCS SP5; Leica Microsystems, Mannheim, Germany).

3.6. Cell culture and in vitro splicing assay

HEK 293T cells were maintained in high glucose-DMEM supplemented with 100 U/mL penicillin, 100 μg/mL streptomycin, and 10% FBS. The *GHRHR* exons 2–3 and their flanking intronic sequences (929-bp) were amplified by PCR from the DNA of the patient and a control subject using the following set of primers: GHRHR-Ex2-3-Up_*Xho*I, 5′-ggctcgagtttTCGGTCAACCCTAACCTCTG-3′, and GHRHR-Ex2-3-Lo_BamHI, 5′-ccggatcctttGGCTTCTGCTAACACCTGGA-3′ (the lowercase letters indicate a linker sequence containing *Xho*I and *Bam*HI sites [underlined], respectively). The resulting purified amplicons were digested and subcloned into the *Xho*I/*Bam*HI site of the exon-trapping vector pSPL3 (Invitrogen), and designated as pSPL3-GHRHR-Ex2-3-WT or -mutant (IVS2 + 3a > g). The integrity of the constructed plasmid was confirmed by direct sequencing. Splicing assays were performed in HEK 293T cells transfected with 1 μg of the plasmid. Duplicate independent transfections were carried out. Forty-eight hours later, total RNA was isolated and first-strand cDNA was synthesized from 500 ng of total RNA. The resulting 2.5 ng of cDNA (assuming 100% conversion of RNA to cDNA during the reverse transcription step) was amplified, with the primer combination SD6 and SA2 (vector-specific primer set). Amplification of β-actin mRNA (101-bp) (ACTB_ex3F: 5′-AAGGCCAACCGCGAGAAG-3′; ACTB_ex4R: 5′-CCAGAGGCGTACAGGGATAG-3′) was used to assess the reaction efficiency. In addition, RT-PCR products were purified and subcloned into a pCR4-TOPO TA vector (Invitrogen). Approximately 50 individual plasmid clones were randomly selected, and the purified plasmid DNAs were analyzed by *Eco*RI digestion and sequencing using universal M13 primers and a BigDye Terminator v3.1 Cycle Sequencing Kit on an ABI

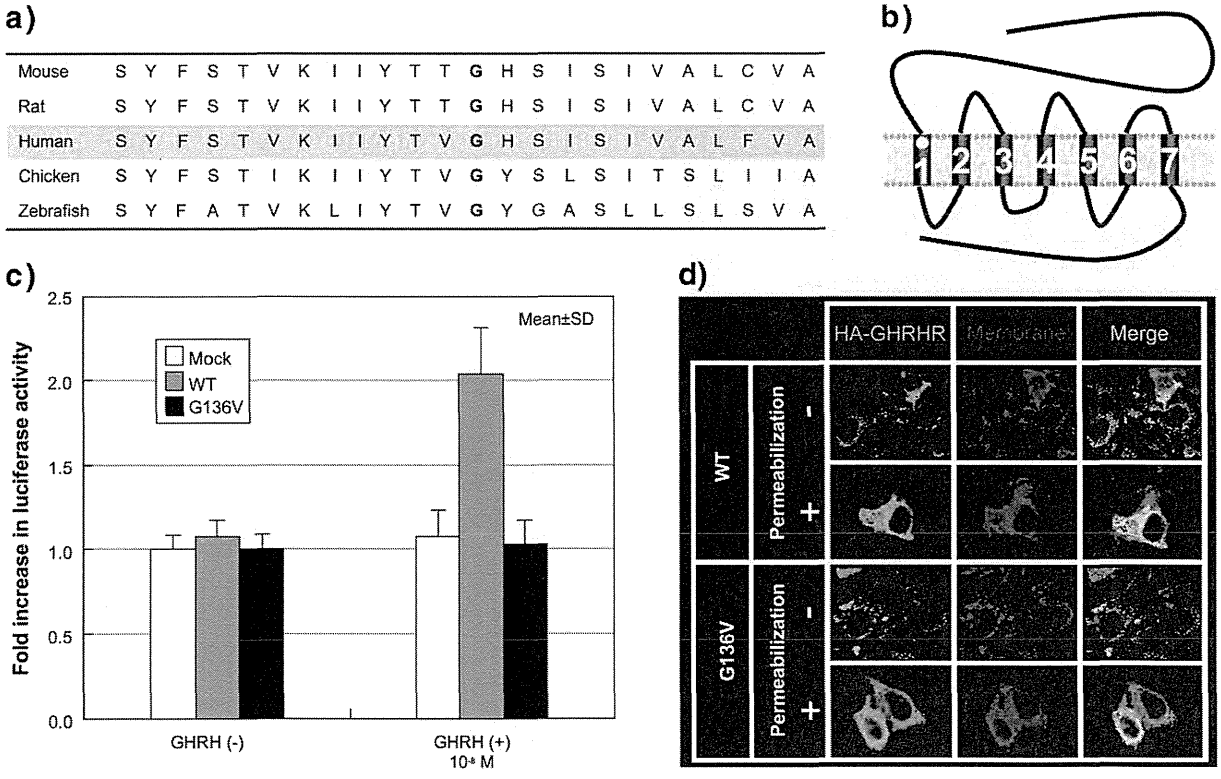

Fig. 2. Delineation of the *G136V* mutation. a) Evolutionary conservation of the 136th glycine among diverse species. b) Schematic representation of the GHRHR protein; the 136th glycine resides in the first transmembrane domain of the receptor. c) Basal and GHRH-stimulated intracellular luciferase activity levels in HEK293 cells transiently transfected with GHRHR. The bars represent the negative control (left, lipofectamine alone), wild-type GHRHR (middle), and G136V mutant GHRHR (right). The assay was conducted in quadruple. d) Subcellular localization analyses using hemagglutinin (HA)-tagged GHRHR constructs. Wild type (WT) and G136V receptors showed comparable surface distribution of fluorescence, indicating equivalent membrane receptor expression.

Prism 3130xl genetic analyzer. Sequence data were assembled into contigs using the SeqMan II program (DNASTAR®, Madison, WI).

3.7. Bioinformatics

To evaluate the effects of *GHRHR* IVS2 + 3a > g substitution on 5′-splice donor site strength, we used 5 web-based tools for splice-site analysis: the Splice Site Prediction by Neural Network (NN; http://www.fruitfly.org/seq_tools/splice.html), the Splice-Site Analyzer Tool (SS; http://ibis.tau.ac.il/ssat/SpliceSiteFrame.htm), the SD-Score Algorithm (SD, http://www.med.nagoya-u.ac.jp/neurogenetics/SD_Score/sd_score.html), the MaxEntScan score5ss program (http://genes.mit.edu/burgelab/maxent/Xmaxentscan_scoreseq.html), and the HBond (Hydrogen Bond) Score Web-Interface (HBond, http://www.uni-duesseldorf.de/rna/html/hbond_score.php).

3.8. Ethical considerations

The patient's parents provided written informed consent for the genetic studies described above. The Ethical Committee of Kanagawa Children's Medical Center reviewed and approved the study procedures.

4. Results

4.1. Pharmacological GH stimulation tests

The patient showed impaired GH responses. GH peaked at 2.81 ng/mL in response to insulin-induced hypoglycemia, 3.78 ng/mL in response to arginine, 3.93 ng/mL in response to GHRH, and 1.35 ng/mL in response to GH-releasing peptide-2 (GHRP-2; [22,23]). The normal response to the above pharmacological stimulants is defined as above 6 ng/mL, except for GHRP-2, where normal response is defined as above 16 ng/mL [22].

4.2. Mutation detection

In the *GH-1* gene, no pathological mutations were identified. Sequencing of the *GHRHR* gene revealed compound heterozygous mutations consisting of a G to T transition in the 407th nucleotide in the 5th exon, substituting glycine (GGC) with valine (GTC) [p.G136V], and an A to G transition at position 3 in IVS 2 [IVS2 + 3a > g]. Her father was found to be heterozygous for p.G136V, while her mother was heterozygous for IVS2 + 3a > g (Fig. 1b). Neither mutation has been previously reported, nor were they found in 150 Japanese control individuals. The MLPA analysis did not detect any deletion or duplication at the exon level in each gene examined.

4.3. Functional characterization of the missense mutation in GHRHR (p.G136V)

The glycine to valine mutation at position 136 of the *GHRHR* gene is located in the first transmembrane-spanning domain, and is conserved in disparate species such as mouse, rat, chicken, and zebrafish (Fig. 2a,b). The effect of p.G136V was evaluated by GHRH-induced luciferase reporter assay. Fig. 2c shows that GHRH-stimulated luciferase activity was significantly impaired in p.G136V-GHRHR than in WT cells. HA-tagged WT and G136V receptors showed comparable surface distribution of fluorescence, indicating equivalent membrane receptor expression (Fig. 2d).

4.4. Bioinformatics

To predict the effects of the *GHRHR* IVS2 + 3a > g on mRNA splicing, we first used 5 in silico programs (Table 1). In general, these assessments predicted the intrinsic strength of the 5′-splice site of the WT sequence to be relatively low (NN = 0.31 and SS = 71.6,

Table 1
Comparison of 5′-splice donor sites.

	Position									Splice Site Prediction by Neural Network	Splice-site analyzer tool			SD-score algorithm		MaxEntScan::score5ss[a]				HBond score web-interface
	−3	−2	−1	+1	+2	+3	+4	+5	+6	Score	Score	No. of H-Bond between U1 and 5′ splice-site	Free energy of U1/5′ splice-site pairing	SD-score	Coefficient of variation	ME model	MDD Model	FM model	WM model	H-Bond score
Wild	*T*	*G*	*G*	*g*	*t*	*a*	*t*	*g*	*g*	0.31	71.63	7	−4.7	−3.46	0.72	6.23	8.68	5.39	4.88	11.7
IVS2 + 3a > g	*T*	*G*	*G*	*g*	*t*	*g*	*t*	*g*	*g*	0.01	66.67	7	−4.4	−4.80	0.68	1.27	7.28	2.07	3.50	8.3
Cryptic donor site1[b]	*C*	*A*	*G*	*g*	*t*	*g*	*g*	*t*	*g*	0.01	67.69	6	−5.8	−4.10	0.69	1.16	8.08	3.35	4.48	11.8
Cryptic donor site2[b]	*G*	*A*	*G*	*g*	*c*	*a*	*g*	*g*	*t*	0.01	69.73	7	−4.7	na	na	1.90	5.42	2.00	1.74	na
U1 snRNA 3′-	G	U	C	C	A	U	U	C	A	−5′										

na: not applicable. U1 snRNA: U(uridine-rich)1 small nuclear ribonucleic acid. Website of each tool used for splice-site analysis is given in the Materials and Method section.
[a] ME, maximum entropy; MDD, maximum dependence decomposition; FM, first-order Markov; WM, weight matrix.
[b] For the location of each cryptic donor site, see Fig. 3d.

calculated using the Neural Network approach and the Shapiro–Senapathy algorithm, respectively), and that IVS2 + 3a > g further reduces the strength (NN = 0.01 and SS = 66.7), potentially leading to aberrant splicing. The latter hypothesis was further corroborated by other methods. For example, based on the SD-score algorithm, the ΔSD-Score of this mutation was calculated as −1.336, and thus was predicted to cause aberrant splicing. A decrease in the HBond score (11.7 to 8.3) also suggested a reduced sequence complementarity to U1 snRNA (small nuclear RNA).

4.5. In vitro splicing assay

The effect of IVS2 + 3a > g on in vitro splicing efficiency was evaluated using minigene constructs, containing the *GHRHR* exons 2 and 3 with either the WT or mutant sequence (Fig. 3a). RT-PCR of the minigenes revealed that the WT construct generated 2 major splicing products of approximately 470- and 600-bp in size, with the former species being dominant (Fig. 3b). Subcloning and subsequent sequencing showed that the predominant lower band consisted of the expected normal splicing product of 471-bp containing exons 2 and 3 as well as the 474-bp product generated by alternative usage of a CAGCAG tandem acceptor of IVS1, and that the upper band consisted of spliced products but retained the 126-bp sequence of IVS2 (Fig. 3c).

The IVS2 + 3a > g construct also produced 2 bands (Fig. 3b, lane 4), with the 600-bp fragment being the predominant band (Fig. 3b,c). The smaller band (Fig 3b, lane 4) contained either an intronic 20- or 16-bp insertion, consistent with aberrant splicing events due to utilization of cryptic donor splice sites within intron 2 (Fig. 3d, Table 1). The 471/474-bp clones, reflective of normal splicing, were not detected.

Notably, comparison with reference human genomic sequences indicated that the 20-bp-inserted clones used the canonical (gt–ag) splice-site pair, whereas the 16-bp-inserted clones used a non-canonical (gc–ag) splice-site pair (Fig. 3d). In addition, several splicing prediction algorithms (e.g., SS and SD) showed higher 5′-splice site strength for these cryptic splice sites, compared to the mutated counterpart (Table 1). Taken together, our data suggested that IVS2 + 3a > g results in a significant decrease in normal splicing efficiency as well as the activation of cryptic donor splice sites.

5. Discussion

The phenotype of human *GHRHR* gene mutation is IGHD with autosomal recessive trait, classified as IGHD type 1B. First described in 1996 [17], more than 20 mutations have been reported, including a mutation in a POU1F1-binding site of the promoter region [24], missense mutations [8–11,24,25], nonsense mutations [7,8,12,26–28], microdeletions [13,25,29], and splice site mutations [6,14–16,19,26,30–33] (Table 2). Most cases were reported to be severely GH deficient, with extremely low IGF-1 levels and profoundly diminished GH responses to the pharmacological stimulants. Anterior pituitary hypoplasia was a common finding.

This report describes novel compound heterozygous mutations in the *GHRHR* gene in an IGHD patient without consanguinity. The first mutation was a G to T transition in the 407th nucleotide located in

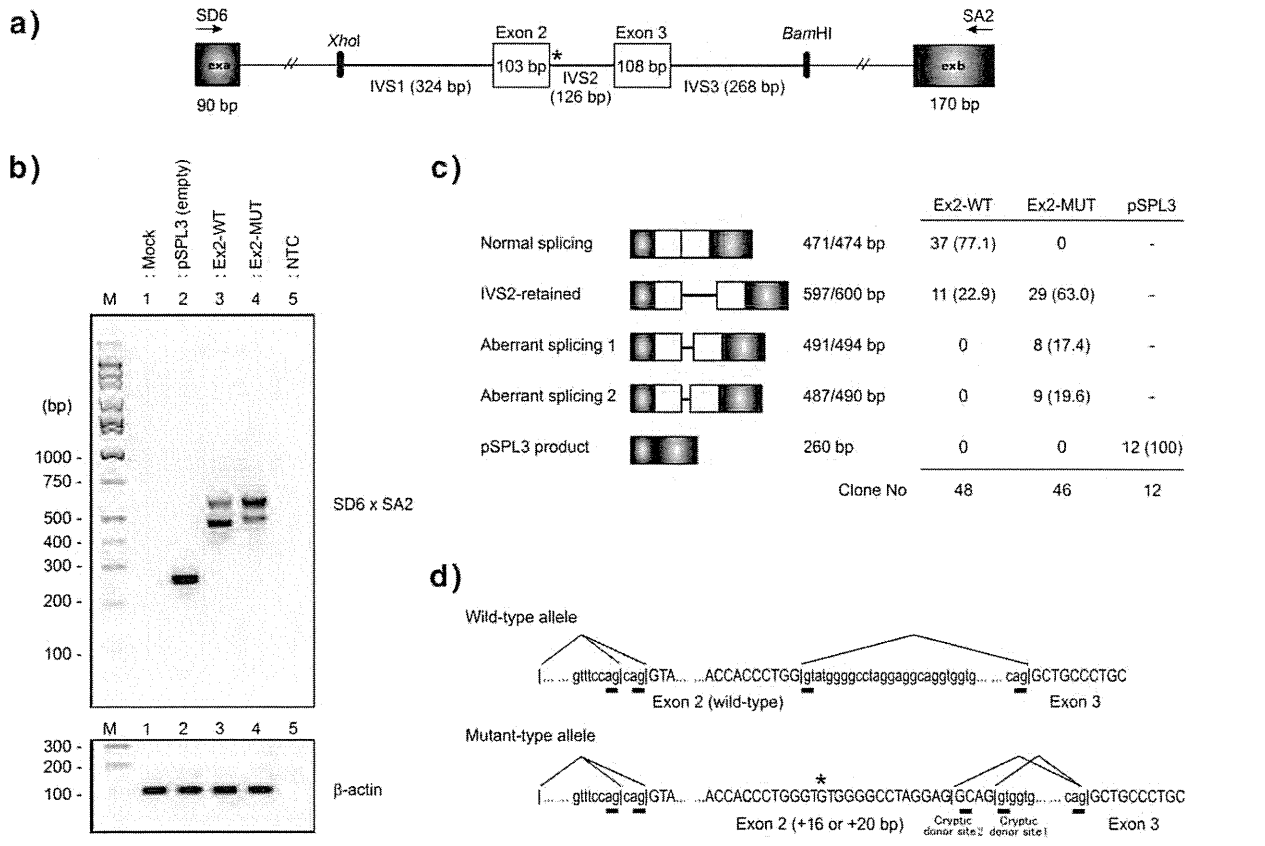

Fig. 3. In vitro splicing assay to verify the effect of the *IVS2 + 3a > g* mutation. a) Schematic diagrams of the *GHRHR* gene locus around the *IVS2 + 3a > g* mutation and the minigene constructs for in vitro splicing assay. SD6 and SA2 are exon-trapping vector pSPL3-specific primers. b) RT-PCR amplification of the GHRHR transcripts obtained from cells transfected with the plasmids pSPL-3-empty (lane 2), pSPL-3-GHRHR exons 2 and 3 wild type (WT; lane 3), pSPL-GHRHR exons 2 and 3 mutant (lane 4), and non-template control (NTC; lane 5). c) Schematic diagrams of WT, various aberrant splicing products, and the appearance frequency. Depending on the alternative usage of CAGCAG tandem in IVS1 acceptor site, the length of normal splice product was either 471 or 474 bp. d) Schematic representation of normal splicing and aberrant splicing with the cryptic 5′ splice sites usage. Underlined nucleotides indicate that both the authentic and cryptic splice sites are involved.

Table 2
Summary of the hitherto reported human mutations in the *GHRHR* gene.

Mutation (site)	Domain	Ethnicity	Consanguinity	Gender	Age at investigation	Height (SDS)	Peak GH response to pharmacological stimuli (ng/mL)					IGF-1 (ng/mL)	IGFBP3 (μg/mL)	Hypoplastic pituitary on MR imaging (age)	Ref.
							GHRH	insulin	arginine	L-DOPA	clonidine				
−124A > C (promotor) K329F (exon 11)	promoter 3rd IC loop	U	−	M	4y	−4.6	1.6	1.2						+ (4 y)	24
IVS1 + 1G > A/IVS1 + 1G > A		Brazil	+	M9, F13	5y − 20y (n = 22)	−2.7 – −8.4	0.63 ± 0.61	flat			flat	6.7 ± 2.8	0.43 ± 0.17	ND	6
IVS1 + 1G > A/IVS4-2A > G		Brazil	−	F	9.5 y	−6.2		1.5			1.9			+ (9 y)	16,30
IVS1 + 1G > A/ E382E (exon 12)		Brazil	−	F	7.1 y	−3.3		0.1						+ (16 y)	16
IVS1 + 2 T > G/IVS1 + 2 T > G		Morroco	+	M F	11y6m 9y4m	−6.6 −4.4		0.1 4.2		0.1 1.2		21 17.4		+ (14 y) + (9 y)	15
Q43X (exon 2) IVS3 + 1G > A	1st EC domain	U	−	M M	11y 8y9m	−5.5 −5.5	<0.05 <0.05		<0.05 <0.05		<0.05 <0.05	20 16		+ (20 y) + (18 y)	26
E72X/E72X (exon 3)	1st EC domain	Sri Lanka	−	M M	7.7 y 6.9 y	−4 −5	<1.5 <1.5					<38.5 <38.5		+ (10 y) + (9 y)	27
		Pakistan	+	M14, F3	3 y – 28 y (n = 17)	−7.2 ± 1.18	0.107 ± 0.053			0.255 ± 0.193	0.374 ± 0.406	5.2 ± 2.0 (n = 14)	0.42 ± 0.13 (n = 14)	ND	7
		U	U	F F	13.8 y 14.8 y	−8.6 −6.74		0.1 0.0		0.1 0.2		7.5 4.2	0.626 0.612	+ (13 y) + (14 y)	28
		India	+ in 2/5 families	M8, F5	4y – 17 y	−4.1 – −8.6	<0.96 (n = 7)			0.9, 1.0	<3.2 (n = 10)	10 – 15 (n = 4)	0.38, 0.42	+ in 4/4 + (4 y – 13 y)	12
		Asia/ Somalia	+	M4, F4	3 y – 15 y (n = 6)	−2.33 – −6.64		<0.1 – 2.2[a]				<−2.5SDS		+ (n = 6) − (n = 2; 4 y, 6 y)	8
E72X/R161W (exon6)	EC/1st IC loop	Asia Asia	−	M F	5.2 y 4.9 y	−4.81 −4.48		0.7[a] 0.6[a]				<−3.5SD <−2.5SD		+ (5 y) − (4 y)	
R94L/R94L (exon4)	1st EC domain	Asia	U	F	5.8 y	−5.6		0.9[a]				−3.0SD		+ (5 y)	

391delG/391delG (exon4)	1st EC domain	Egypt	+	F	5.9 y	−5.5		0.3		0.3	9		+ (5 y)	13
				F	5.9 y	−5.74					<6		− (4 y)	
				F	5.9 y	−6.01					<6		+ (5 y)	
H137L (exon 5) del 1140-1144 (exon11)	1st TM 7th TM	U	−	F	14 y 2m	−7.0	1.0						ND	25
				M	11 y 6m	−5.9	1.0						ND	
L144H/L144H (exon 5)	1st TM	Spain	−	M	5 y	−4.0	0.41				22		+ (5 y)	9
				M	3 y	−3.3	2.0				40		ND	
		Brazil	+	F	26 y	−7.4	<0.3				4.6		+ (26 y)	10
				F	19 y	−7.1	<0.3				2.5		+ (19 y)	
L144H/F242C (exon 7)	1st TM/ 4th TM	US	−	M	17 y 6m	−5.2	3.8						ND	9
				M	16 y 2m	−4.5	2.3						ND	
A176V/A176V (exon6)	2nd TM	Pakistan	+	M	8.5 y	−4.5	<1 mU/L	1.2 mU/L					+ (8 y)	11
				M	8.4 y	−3.5		2.0 mU/L					+ (8 y)	
A222E/A222E (exon 7)	3rd TM	Pakistan	+	M	11 y 2m	−6.8							ND	9
				M	2 y10m	−5.2							ND	
		Asia	+	M	3.2 y	−2.8		0.4[a]			<−3.5SD		+ (3y)	8
				F	2.0 y	−2.98		0.4[a]			<−3.5SD		ND	
IVS7 + 1G > C/IVS7 + 1G > C		Morroco	−	M	16 y	−5.1	absent	5.0 mU/L			14.5		− (25 y)	31,32
				F	14.9 y	−7.3	absent	1.3 mU/L			26.8		− (23 y)	
IVS7-1G > A/IVS7-1G > A		Brazil	+	M	10.1 y	−3.9	2.6			1.3	18		ND	16
				F	3.5 y	−2.5	1.76			3.49			ND	
IVS8 + 1G > A/IVS8 + 1G		China	−	F	56 y	121.2 cm							ND	33
				F	42 y	119.5 cm							+ (42 y)	
				F	36 y	120.2 cm		0.15			31.5	<0.5	+ (36 y)	
W273S/W273S (exon9)	2nd EC loop	Asian	U	F	6.0 y	−4.92					−3.5SD		+ (6 y)	8
		Asian		F	2.6 y	−2.8		0.9[a]			−1.9SD		− (2− y)	
E382E/E382E (exon12)	intracellular tail	Japan	−	F	7 y 2m	−5.2	2.0	2.1					− (7 y)	19
				F	5 y9m	−5.6							− (5 y)	
del 1121-1124/ del 1121-1124 (exon12)	7th TM	Japan	−	M	3 y	−6.0	0.2	0.6	0.8	0.6	67.9		+ (3 y)	29
IVS12 + 2 T > A/IVS12 + 2 T > A		Pakistan	+	M	8 y	−3.6	0.6	0.4			49		− (8 y)	14
				F	3 y	−2.7	0.7	1.7					− (4 y)	
				F	2 y	−2.5	1.0	0.5			41		+ (3 y)	

EC, extracellular; TM, transmembrane; U, unavailable.

[a] The stimulant was either insulin or glucagon.

exon 5, which led to p.G136V substitution. Functional analysis showed that the G136V mutant failed to elicit any discernible luciferase activity increment in response to GHRH stimulation, albeit normal membranous localization in the immunofluorescence study. Salvatori et al. reported a H137L mutation also located in the first GHRHR transmembrane domain and showed that this mutant receptor was normally expressed [25]. In addition, the first transmembrane domain has been shown to be important for ligand binding, both in GHRHR [34] and in the V2 vasopressin receptor [35]. These findings suggest that impairment of receptor function due to p.G136V must occur in the process from ligand binding to cAMP generation.

The second mutation, IVS2 + 3a > g, is an uncommon splice site mutation, considering that both adenosine (A) and guanidine (G) nucleotides are similarly conserved at the +3 position of the 5′-splice donor site in humans. However, several lines of evidence support our assumption that IVS2 + 3a > g is a disease-causing mutation. First, several examples of disease-associated a > g mutations at this position have been previously described [36,37]. In particular, Ohno et al. reported 10 cases of human disease associated with a > g substitutions at the +3 site [37]. Second, all the in-silico programs we utilized predicted that IVS2 + 3a > g would have resulted in aberrant splicing. Lastly, a splicing assay using a mini-gene construct and containing the mutant genomic DNA spanning exons 2 to 3 of the *GHRHR* gene demonstrated that aberrant splicing products, with a 20-bp or 16-bp insertion, were mainly generated from the allele containing the IVS2 + 3a > g mutation. The 20- and 16-bp insertions would cause a frameshift and result in truncated GHRHR with 98 and 107 amino acids, respectively. These truncated GHRHRs would lose biological activity, assuming the protein structures were profoundly altered.

The minigene constructs with both WT and the IVS2 + 3a > g mutant also generated the 600-bp product, which retained the 126-bp sequence of IVS2. According to the prediction tool for transmembrane helices in proteins (TMHMM v2.0: http://www.cbs.dtu.dk/services/TMHMM-2.0), the 600-bp products would produce GHRHR with an extended 42-amino acid sequence on its N-terminal (results not shown). Although the biological activity of the 600-bp (+42 amino acid) GHRHR is uncertain, and it is unknown whether the longer GHRHR would be generated in vivo, it may have some residual function, considering that it is normal structure except for the longer N-terminal.

In the majority of patients described with *GHRHR* gene mutations, GH responses to pharmacological stimulants had been completely or nearly absent (Table 2). However, our patient, despite severe growth failure and low IGF-1 levels, showed significant GH responses to the various stimulants. In particular, exogenous GHRH induced a GH response up to 3.93 ng/mL, which seemed paradoxical. For measuring circulating GH levels, we utilized the RIA kit with recombinant GH molecule as the standard. Therefore, the absolute values of serum GH level tended to be lower compared to the values determined by RIA/IRMA with older standards [21]. Thus, methodological differences in GH measurement cannot explain the significant GH response observed in our patient.

Another possible explanation for the GH response may be the younger age of our patient (2 years). As noted in Table 2, our patient was one of the youngest among the reported cases. In the setting of diminished GHRH stimulation, GH response to pharmacological stimulants may gradually decrease with advancing age. In addition, as suggested previously [38], age-dependent changes may also affect pituitary size in patients with *GHRHR* mutations. Whereas our patient was found to have normal pituitary size, previous morphological studies described hypoplastic pituitaries in patients older than 8 years of age [38]. Further research involving serial GH stimulation tests and MR imaging studies may help clarify the presence of age-dependent decline in GH response and pituitary size.

It is also possible that, unlike the in vitro results, splicing inefficiencies at the cryptic donor sites may result in normal splicing in vivo, albeit at very low frequency, and could account for low detection level of stimulated GH.

Yet another possible explanation for the GH response in our patient may be explained by the presence of the 600-bp GHRHR isoform discussed earlier. The increased expression of this form of GHRHR may result in preservation of some receptor function. In addition, different GHRHR isoforms originating from the 4th exon (359 and 337 amino acids) have been reported [39]. Given that these isoforms must also be generated in our patient, it may be the case that they exert some receptor functions.

The parents of our patient harboring heterozygous *GHRHR* mutation had normal stature. This finding is in accordance with other reports arguing against any effects of heterozygosity, although gene–dosage effect [7] or dominant negative effect [29,40] of the mutant *GHRHR* had been suggested previously.

In conclusion, we identified novel compound heterozygous *GHRHR* gene mutations in a Japanese IGHD patient without consanguinity. Although the clinical manifestation was compatible with severe GH deficiency, GH reactivity against pharmacological stimuli including GHRH was partially preserved. To elucidate this mechanism, re-testing after a significant time interval may be helpful.

Conflict of interest statement

The authors declare that they have no conflicts of interest.

Acknowledgment

We thank Ms. Yukiko Yamashita-Sakamoto from The University of Tokushima for her excellent technical assistance.

References

[1] K.A. Lacey, J.M. Parkin, Causes of short stature. A community study of children in Newcastle upon Tyne, Lancet 1 (1974) 42–45.
[2] R. Lindsay, M. Feldkamp, D. Harris, et al., Utah Growth Study: growth standards and the prevalence of growth hormone deficiency, J. Pediatr. 125 (1994) 29–35.
[3] M. Thomas, G. Massa, M. Craen, et al., Prevalence and demographic features of childhood growth hormone deficiency in Belgium during the period 1986–2001, Eur. J. Endocrinol. 151 (2004) 67–72.
[4] G.V. Vimpani, A.F. Vimpani, G.P. Lidgard, et al., Prevalence of severe growth hormone deficiency, Br. Med. J. 2 (1977) 427–430.
[5] L.A. Pérez Jurado, J. Argente, Molecular basis of familial growth hormone deficiency, Horm. Res. 42 (1994) 189–197.
[6] R. Salvatori, C.Y. Hayashida, M.H. Aguiar-Oliveira, et al., Familial dwarfism due to a novel mutation of the growth hormone-releasing hormone receptor gene, J. Clin. Endocrinol. Metab. 84 (1999) 917–923.
[7] H.G. Maheshwari, B.L. Silverman, J. Dupuis, et al., Phenotype and genetic analysis of a syndrome caused by an inactivating mutation in the growth hormone-releasing hormone receptor: dwarfism of Sindh, J. Clin. Endocrinol. Metab. 83 (1998) 4065–4074.
[8] K.S. Alatzoglou, J.P. Turton, D. Kelberman, et al., Expanding the spectrum of mutations in GH1 and GHRHR: genetic screening in a large cohort of patients with congenital isolated growth hormone deficiency, J. Clin. Endocrinol. Metab. 94 (2009) 3191–3199.
[9] R. Salvatori, X. Fan, J.A. Phillips III, et al., Three new mutations in the gene for the growth hormone (GH)-releasing hormone receptor in familial isolated GH deficiency type IB, J. Clin. Endocrinol. Metab. 86 (2001) 273–279.
[10] R. Salvatori, M.H. Aguiar-Oliveira, L.V. Monte, et al., Detection of a recurring mutation in the human growth hormone-releasing hormone receptor gene, Clin. Endocrinol. (Oxf.) 57 (2002) 77–80.
[11] M. Carakushansky, A.J. Whatmore, P.E. Clayton, et al., A new missense mutation in the growth hormone-releasing hormone receptor gene in familial isolated GH deficiency, Eur. J. Endocrinol. 148 (2003) 25–30.
[12] T. Kamijo, Y. Hayashi, H. Seo, et al., A nonsense mutation (E72X) in growth hormone releasing hormone receptor (GHRHR) gene is the major cause of familial isolated growth hormone deficiency in Western region of India: founder effect suggested by analysis of dinucleotide repeat polymorphism close to GHRHR gene, Growth Horm. IGF Res. 14 (2004) 394–401.
[13] R. Shohreh, R. Sherafat-Kazemzadeh, Y.H. Jee, A novel frame shift mutation in the GHRH receptor gene in familial isolated GH deficiency: early occurrence of anterior pituitary hypoplasia, J. Clin. Endocrinol. Metab. 96 (2011) 2982–2986.
[14] M. Alba, C.M. Hall, A.J. Whatmore, et al., Variability in anterior pituitary size within members of a family with GH deficiency due to a new splice mutation in the GHRH receptor gene, Clin. Endocrinol. (Oxf.) 60 (2004) 470–475.

[15] L. Hilal, Y. Hajaji, M.P. Vie-Luton, et al., Unusual phenotypic features in a patient with a novel splice mutation in the GHRHR gene, Mol. Med. 14 (2008) 286–292.
[16] S. Marui, E.B. Trarbach, M.C.S. Boguszewski, et al., GH-releasing hormone receptor gene: a novel splice-disrupting mutation and study of founder effects, Horm. Res. Paediatr. 78 (2012) 165–172.
[17] M.P. Wajnrajch, J.M. Gertner, M.D. Harbison, et al., Nonsense mutation in the human growth hormone-releasing hormone receptor causes growth failure analogous to the little (lit) mouse, Nat. Genet. 12 (1996) 88–90.
[18] L.C. de Graaff, J. Argente, D.C. Veenma, et al., Genetic screening of a Dutch population with isolated GH deficiency (IGHD), Clin. Endocrinol. (Oxf.) 70 (2009) 742–750.
[19] H. Inoue, N. Kangawa, A. Kinouchi, et al., Japan Growth Genome Consortium: identification and functional analysis of novel human growth hormone-releasing hormone receptor (GHRHR) gene mutations in Japanese subjects with short stature, Clin. Endocrinol. (Oxf.) 74 (2011) 223–233.
[20] T. Tanaka, S. Yokoya, N. Kato, et al., The Journal of the Japan Pediatric Society (in Japanese), 115 (2011) 1705–1709, (available at http://jspe.umin.jp/pdf/taikakushisuv2.xlsx).
[21] T. Tanaka, K. Tachibana, A. Shimatsu, et al., A nationwide attempt to standardize growth hormone assays, Horm. Res. 64 (Suppl.) (2005) 6–11.
[22] Y. Asakura, Y. Toyota, K. Muroya, et al., Growth hormone response to GH-releasing peptide-2 in children, J. Pediatr. Endocrinol. Metab. 23 (2010) 473–480.
[23] K. Chihara, A. Shimatsu, N. Hizuka, et al., KP-102 study group: a simple diagnostic test using GH-releasing peptide-2 in adult GH deficiency, Eur. J. Endocrinol. 157 (2007) 19–27.
[24] R. Salvatori, X. Fan, P.E. Mullis, et al., Decreased expression of the GHRH receptor gene due to a mutation in a Pit-1 binding site, Mol. Endocrinol. 16 (2002) 450–458.
[25] R. Salvatori, X. Fan, J.A. Phillips III, et al., Isolated growth hormone (GH) deficiency due to compound heterozygosity for two new mutations in the GH-releasing hormone receptor gene, Clin. Endocrinol. (Oxf.) 54 (2001) 681–687.
[26] R. Salvatori, X. Fan, J.D. Veldhuis, et al., Serum GH response to pharmacological stimuli and physical exercise in two siblings with two new inactivating mutations in the GH-releasing hormone receptor gene, Eur. J. Endocrinol. 147 (2002) 591–596.
[27] I. Netchine, P. Talon, F. Dastot, et al., Extensive phenotypic analysis of a family with growth hormone (GH) deficiency caused by a mutation in the GH-releasing hormone receptor gene, J. Clin. Endocrinol. Metab. 83 (1998) 432–436.
[28] Z. Sıklar, M. Berberoğlu, M. Legendre, et al., Two siblings with isolated GH deficiency due to loss-of-function mutation in the GHRHR gene: successful treatment with growth hormone despite late admission and severe growth retardation, J. Clin. Res. Pediatr. Endocrinol. 2 (2010) 164–167.
[29] R. Horikawa, Isolated GH deficiency due to inactivating mutation of GHRH receptor. [In Japanese], Nihonrinsho 60 (2002) 297–305.
[30] M.G.F. Osorio, S. Marui, A.A.L. Jorge, et al., Pituitary imaging and function in patients with growth hormone deficiency with and without mutations in GHRH-R, GH-1, or PROP-1 genes, J. Clin. Endocrinol. Metab. 87 (2002) 5076–5084.
[31] F. Roelfsema, N.R. Biermasz, R.G. Veldman, et al., Growth hormone (GH) secretion in patients with an inactivating defect of the GH-releasing hormone (GHRH) receptor is pulsatile: evidence for a role for non-GHRH inputs into the generation of GH pulses, J. Clin. Endocrinol. Metab. 86 (2001) 2459–2464.
[32] M.J.E. Walenkamp, A.M. Pereira, W. Oostdijk, et al., Height gain with combined growth hormone and gonadotropin-releasing hormone analog therapy in two pubertal siblings with a growth hormone-releasing hormone receptor mutation, J. Clin. Endocrinol. Metab. 93 (2008) 204–207.
[33] Q. Wang, Y. Diao, Z. Xu, et al., Identification of a novel splicing mutation in the growth hormone (GH)-releasing hormone receptor gene in a Chinese family with pituitary dwarfism, Mol. Cell. Endocrinol. 313 (2009) 50–56.
[34] V.I. DeAlmeida, K.E. Mayo, Identification of binding domains of the growth hormone-releasing hormone receptor by analysis of mutant and chimeric receptor proteins, Mol. Endocrinol. 12 (1998) 750–765.
[35] Y. Pan, P. Wilson, J. Gitschier, The effect of eight V2 vasopressin receptor mutations on stimulation of adenylyl cyclase and binding to vasopressin, J. Biol. Chem. 269 (1994) 31933–31937.
[36] R. Kan, S.R. Twigg, J. Berg, et al., Expression analysis of an FGFR2 IIIc 5′ splice site mutation (1084 + 3A → G), J. Med. Genet. 41 (2004) e108.
[37] K. Ohno, J.M. Brengman, K.J. Felice, et al., Congenital end-plate acetylcholinesterase deficiency caused by a nonsense mutation and an A → G splice-donor-site mutation at position +3 of the collagenlike-tail-subunit gene (COLQ): how does G at position +3 result in aberrant splicing? Am. J. Hum. Genet. 65 (1999) 635–644.
[38] H.A. Oliveira, R. Salvatori, M.P. Krauss, et al., Magnetic resonance imaging study of pituitary morphology in subjects homozygous and heterozygous for a null mutation of the GHRH receptor gene, Eur. J. Endocrinol. 148 (2003) 427–432.
[39] H. Kiaris, I. Chatzistamou, A.V. Schally, et al., Ligand-dependent and -independent effects of splice variant 1 of growth hormone-releasing hormone receptor, Proc. Natl. Acad. Sci. U. S. A. 100 (2003) 9512–9517.
[40] R. Horikawa, K. Fujita, R. Nakajima, et al., A novel growth hormone-releasing hormone (GHRH) receptor mutation as a cause for isolated GH deficiency: its functional analysis, Clin. Pediatr. Endocrinol. 9 (2000) 115.

Clin Pediatr Endocrinol 2013; 22(4), 53–64

Original Article

Abnormal Adipose Tissue Distribution with Unfavorable Metabolic Profile in Five Children Following Hematopoietic Stem Cell Transplantation: A New Etiology for Acquired Partial Lipodystrophy

Masanori Adachi[1], Yumi Asakura[1], Koji Muroya[1], Hiroaki Goto[2], and Hisato Kigasawa[2]

[1]*Department of Endocrinology and Metabolism, Kanagawa Children's Medical Center, Yokohama, Japan*

[2]*Department of Hematology and Regenerative Medicine, Kanagawa Children's Medical Center, Yokohama, Japan*

Abstract. We report five consecutive patients who underwent hematopoietic stem cell transplantation (HSCT) to treat leukemia or neuroblastoma early in their lives and later manifested abnormal patterns of adipose tissue distribution. Lipoatrophy was remarkable in the gluteal regions and extremities, whereas subcutaneous fat was preserved in the cheeks, neck, and abdomen. In addition, visceral fat deposition, fatty changes in the liver, and metabolic derangements such as insulin resistance and hypertriglyceridemia were evident. These features resemble Dunnigan-type familial partial lipodystrophy, which is a rare condition caused by *LMNA* gene mutation. These patients shared a common medical history involving HSCT, including conditioning with total body irradiation (TBI). They also received intensive chemotherapy because of multiple metastases (n = 3), relapse (n = 3), and repetitive HSCT (n = 3). We propose HSCT as a new etiology for acquired partial lipodystrophy and recommend that patients who undergo HSCT with TBI and intensive chemotherapy early in their lives must receive careful observation for the possible development of lipodystrophy and metabolic complications.

Key words: chemotherapy, dyslipidemia, hypertriglyceridemia, insulin resistance, total body irradiation

Introduction

Partial lipodystrophy refers to a pathological and unique fat distribution, characterized by lipoatrophy (loss of adipose tissue) and lipohypertrophy (abnormal fat accumulation) (1, 2). Metabolic complications such as insulin resistance, diabetes, hypertriglyceridemia, and fatty changes in the liver are additional hallmarks of partial lipodystrophy (1–4).

Familial partial lipodystrophy (FPLD) arises from genetic mutations, including mutations in the *LMNA* (5–7), *PPARγ* (8–10), *AKT2* (11) and *CIDEC* (12) genes. Specifically, FPLD caused by a *LMNA* mutation is referred to as Dunnigan-type FPLD, or FPLD2, and is characterized by lipoatrophy in the extremities and buttocks combined with fat accumulation in the face, neck

Received: May 31, 2013
Accepted: July 1, 2013
Corresponding author: Dr. Masanori Adachi, Department of Endocrinology and Metabolism, Kanagawa Children's Medical Center, 2-138-4 Mutsukawa, Minami-ku, Yokohama 232-8555, Japan
E-mail: madachi@mars.sannet.ne.jp

and intra-abdominal areas. Among the acquired forms of partial lipodystrophy, the most prevalent one is highly active antiretroviral therapy (HAART)-associated lipodystrophy syndrome found in HIV-infected individuals (13, 14). Acquired partial lipodystrophy can also develop following viral infection, autoimmune disease or membranous proliferative glomerulonephritis (1).

We treated 5 consecutive patients who had previously undergone hematopoietic stem cell transplantation (HSCT) to treat malignancies at a younger age. These patients, later in their lives, manifested aberrant fat distribution patterns similar to those occurring in patients with FPLD2, as well as severe metabolic abnormalities.

Case Series

All the study procedures, including the control subjects in body composition analysis, were reviewed and approved by the ethics committee of Kanagawa Children's Medical Center. Patients 2, 3, 4, and 5 and the mother of patient 1 provided written informed consent for publication of their facial photographs.

Patient 1, female, acute myeloid leukemia (AML)

As a result of an evaluation of walking difficulties and repetitive, febrile episodes, a 1-yr-old girl was diagnosed with AML, classified as M4, with multiple extra-marrow involvements, including the central nervous system. Following successful induction chemotherapy, bone marrow transplantations (BMTs) from her mother were attempted twice, but were rejected. A third allogeneic BMT, with conditioning that included total body irradiation (TBI) of 10 Gy, was successful and resulted in long-term remission. However, the patient developed chemotherapy-related leukoencephalopathy, and suffered from intractable epilepsy. To suppress extensive, chronic, graft-versus-host disease (GVHD) (15), she had received steroid therapy for 3 yr (Table 1).

At 17 yr of age, the patient underwent her first endocrinological evaluation (Table 2) because she was short [130.3 cm, −5.3 SD for Japanese standards (16)] and prepubertal. Subcutaneous fat was rather abundant in her cheeks and neck, which resulted in a moon-face appearance (Fig. 1a). In addition, the patient exhibited remarkable abdominal distension, with an abdominal circumference of 69 cm at the navel level. However, both her extremities and buttocks showed marked reductions in subcutaneous fat tissue (Fig. 1b).

An oral glucose tolerance test (OGTT) showed a diabetic blood glucose pattern with tremendous hyperinsulinism (Fig. 2). Mildly elevated alanine aminotransferase (ALT) (56 IU/L) and γ glutamyl transpeptidase (γ GTP) (387 IU/L) levels were found, and fatty changes in the liver were suspected based on abdominal ultrasonography (US). Dyslipidemia was also evident, with fasting triglyceride (TG) levels of 675 mg/dL, high-density lipoprotein cholesterol (HDL-C) of 39 mg/dL and low-density lipoprotein cholesterol (LDL-C) of 168 mg/dL (Table 3).

A magnetic resonance imaging scan revealed a small pituitary gland, and the patient was found to have GH deficiency, subclinical hypothyroidism (TSH, 5.45 μIU/L; free T4, 0.93 ng/dL), and primary ovarian insufficiency (FSH, 60.9 IU/L) (Tables 1 and 2).

Patient 2, female, AML

An 8-yr-old girl was diagnosed with AML (M2) through an evaluation for petechiae and epistaxis. Six mo after the first remission was achieved by chemotherapy, a marrow relapse was found. A BMT from a human leukocyte antigen (HLA)-identical donor was conducted, following conditioning that included TBI of 12 Gy. Chronic GVHD with pneumonitis, joint contractures and liver dysfunction required immunosuppressive treatment lasting more than a decade. She also suffered from right-sided femoral neck necrosis (with an onset at age 12), transient aplastic anemia following a parvovirus infection (at age 13) and multiple hepatic angiomas (at age 17).

Table 1 Treatment summaries for the original malignancies in the 5 patients

Pt (sex)	Primary disease (onset)	Treatment			Chronic graft-versus-host disease classification and treatment@	Treatment-related complications
		Chemo-therapy*	Radiation (site)	Transplantation (conditioning#)		
1 (F)	AML (1 yr)	VP-16, Ara-C, MIT, THP-ADR, ACR, VCR, MTX (it), HC (it)	ND	Failed 2 consecutive allogeneic BMTs (BSF, VP-16, L-PAM) Successful third allogeneic BMT (TBI 10 Gy, ATG, TT)	Extensive (skin, liver) CsA (for 1.5 yr), PSL (for 3 yr)	GH deficiency (untreated), hypothyroidism (treated from age 17 yr), leukoencephalopathy, epilepsy, primary hypogonadism (treated from age 17 yr)
2 (F)	AML (8 yr)	VP-16, Ara-C, MIT, IDR, MTX (it), HC (it)	ND	Unrelated BMT following marrow relapse (TBI 12 Gy, BSF, L-PAM)	Extensive (lung, joint, liver) PSL (for 12 yr), FK-506 (for 12 yr)	Femoral neck necrosis, aplastic anemia, hepatic angioma, hypothyroidism (treated from age 15 yr), primary hypogonadism (treated from age 19 yr)
3 (M)	ALL (0 yr)	VCR, THP-ADR, L-ASP, MTX, CPM, Ara-C, 6-MP, PSL, DEX	18 Gy (cranial)	2 consecutive allogeneic BMTs following marrow relapse [1) TBI 12 Gy, VP-16, Ara-C, CPM 2) BSF, VP-16, Ara-C,CPM]	Extensive (skin, joint) CsA (for 4 yr), AZA (for 9 yr), PSL (for 12 yr), MTX (for 1 yr)	GH treatment (from age 11 to 17 yr), chronic thyroiditis (no treatment)
4 (M)	NB (1 yr)	CPM, VP-16, THP-ADR, CDDP, CBDCA	23.4 Gy (cranial), 18 Gy (right orbit)	Scheduled PBSCT (TBI 12 Gy, CBDCA, VP-16, L-PAM)	None	Hypothyroidism (treated from age 4 yr), empty sella, GH deficiency (treated from age 14 to 20 yr), hypogonadism (treated from age 18 yr)
5 (F)	NB (1 yr)	CPM, VP-16, THP-ADR, CDDP, DTIC, IFM	19.8 Gy (epigastrium), 30 Gy (right iliac)	2 consecutive autologous BMTs [1) CBDCA, THP-ADR, L-PAM, 2) CBDCA, VP-16, THP-ADR, CPM], allogeneic BMT following regional and marrow relapse (TBI 12 Gy, TT, VP-16)	Extensive (liver, intestine) FK-506 (for 3 yr), PSL (for 3 yr)	GH deficiency (treated from age 11 to 17 yr), primary hypogonadism (treated from age 15 yr), high-frequency deafness, cataract

F, female; M, male; ND, not done; it, intrathecal injection; BMT, bone marrow transplantation; PBSCT, peripheral blood stem cell transplantation; rt, right. *Abbreviations for agents: VP-16, etoposide; Ara-C, cytarabine; MIT, mitoxantrone hydrochloride; THP-ADR, tetrahydropyranyladriamycin; ACR, aclarubicin hydrochloride; VCR, vincristine sulfate; MTX, methotrexate; HC, hydrocortisone; IDR, idarubicin hydrochloride; L-ASP, L-asparaginase; CPM, cyclophosphamide; 6-MP, 6-mercaptopurine; PSL, prednisolone; DEX, dexamethasone; CDDP, cisplatin; CBDCA, carboplatin; DTIC, dacarbazine; IFM, ifosfamide. #BSF, busulfan; L-PAM, melphalan; ATG, antithymocyte globulin; TT, Thio-TEPA; @CsA, cyclosporin A; FK-506, tacrolimus; AZA, azathioprine.

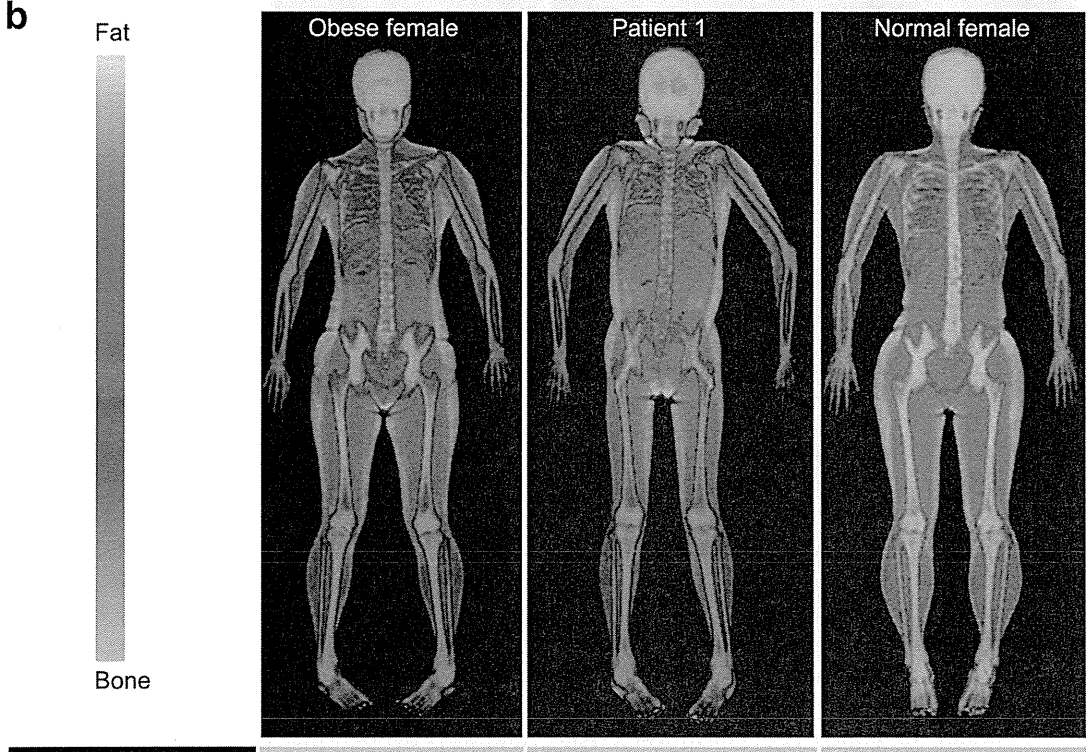

% fat	Obese female	Patient 1	Normal female
upper extremities	54.7	40.5	28.1
trunk	38.5	28.4	18.1
lower extremities	35.0	35.5	30.6
total body	37.2	31.2	23.7

When the patient was 15 yr old, abnormal fat distribution was ascertained by whole body computed tomography (CT) (Fig. 1c). An OGTT showed a normal blood glucose response but with hyperinsulinism (Fig. 2). Dyslipidemia and fatty changes in the liver were also noticed. An endocrinological evaluation revealed mild hypothyroidism (TSH, 9.28 μIU/mL; free T4, 0.89 ng/dL) with primary hypogonadism (FSH, 217.9 IU/L; E2, 5.6 pg/mL).

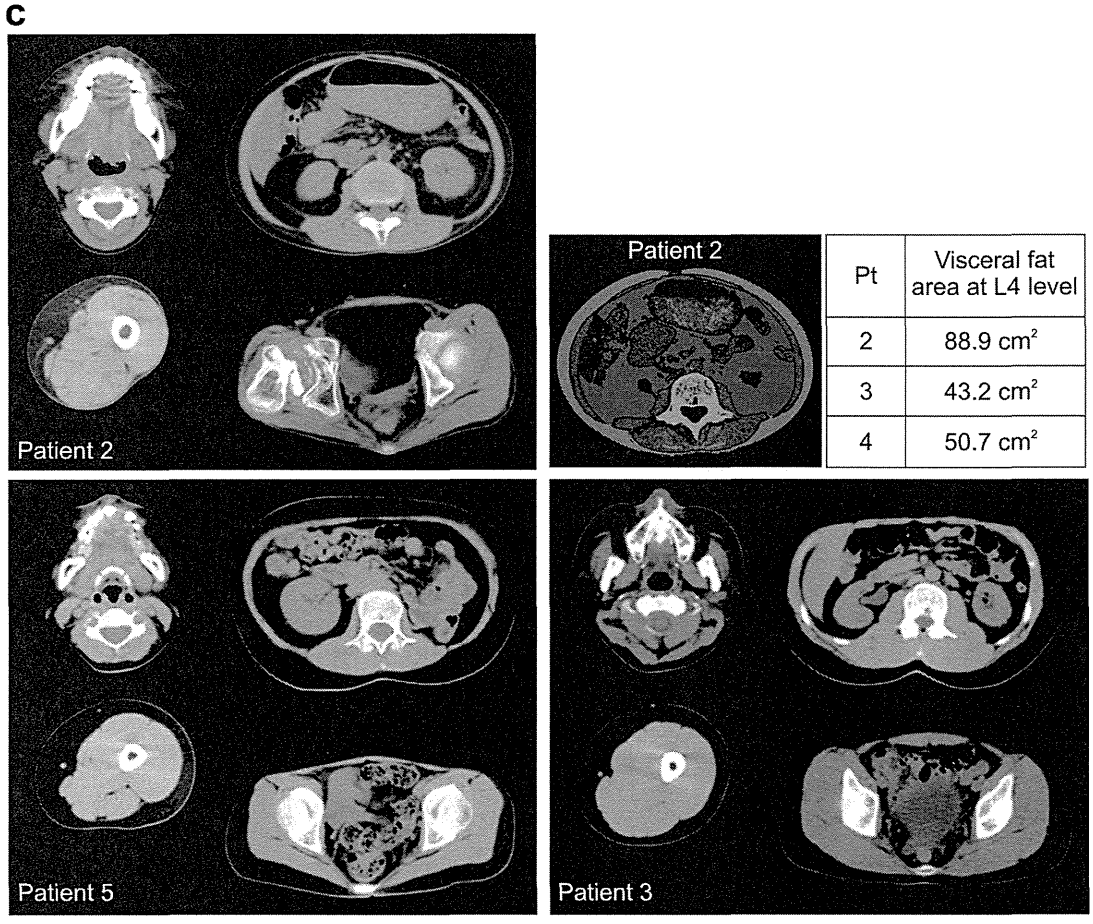

Fig. 1. Abnormal fat distribution observed in the patients. a) Facial photos of the patients. Note that the increased subcutaneous fat tissue in the cheeks gives the impression of a moon-face. b) Dual-energy X-ray absorptiometry image of patient 1 (middle) at age 18 yr. Compared with a 25-yr-old obese woman (left), lipoatrophy in the hips and legs and lipohypertrophy in the neck are evident. For comparison, an image of a nonobese, healthy, 29-yr-old woman is also shown (right). Fat content values of various portions of the body are provided under the images. c) Typical whole-body computed tomography scans of patient 2 at age 18 yr, patient 3 at age 19 yr, and patient 5 at age 18 yr. Increased subcutaneous cheek and visceral fat is evident, whereas loss of subcutaneous fat is remarkable in both the buttocks and thighs. In the inset table, the visceral fat area at the 4^{th} lumbar spine level in each patient is provided, along with the image obtained from patient 2.

Patient 3, male, acute lymphoid leukemia (ALL)

This patient was diagnosed with unclassified ALL at 11 mo of age as a result of an evaluation of petechiae. His first remission was achieved by chemotherapy and 18 Gy cranial radiation. A year later, marrow relapse was found. Following chemotherapy, two consecutive allogeneic BMTs were conducted, with 12 Gy TBI conditioning being provided before the first round of BMT (Table 1).

Chronic GVHD, with major symptoms of joint contractures and scleroderma, was treated with immunosuppressants. In accordance with

Table 2 Current status and information relevant to the etiology of lipodystrophy in the 5 patients

Patient	Current status			At diagnosis of lipodystrophy				Estimated onset of lipodystrophy* (yr)	*LMNA* mutation
	Age (yr)	BMI (kg/m^2)	Typical fat distribution$^{\$}$	Age (yr)	GH status	Thyroid status	Gonadal status		
1	18	17.7	+	17	Deficient	Hypothyroid	Hypogonadal	11	Absent
2	21	12.2	+	15	Sufficient	Hypothyroid	Hypogonadal	13	Absent
3	23	16.5	+	19	Sufficient$^{\#}$	Euthyroid	Eugonadal	12	Absent
4	21	18.3	+	19	Replacement therapy for 5 yr	Replacement therapy for 15 yr	Replacement therapy for 1 yr	15	ND
5	22	14.1	+	17	Replacement therapy for 5 yr	Euthyroid	Replacement therapy for 2 yr	14	Absent

+, present; BMI, body mass index; ND, not determined. $^{\$}$Typical fat distribution denotes lipoatrophy in the gluteal region and extremities coupled with preserved, or even prominent, subcutaneous fat in the cheeks, neck and abdomen. *Onset of lipodystrophy as deduced from the emergence of an elevated triglyceride level. (For details, refer to the Methods section.) $^{\#}$GH treatment was conducted from 11 to 17 yr of age despite normal GH secretion.

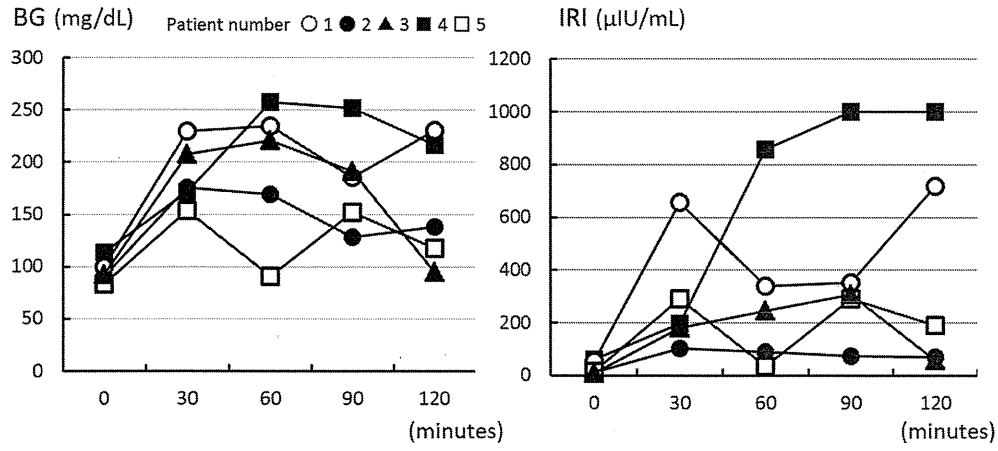

Fig. 2. Results of a 75-g oral glucose tolerance test in the 5 patients. Left panel, blood glucose (BG) response; right panel, insulin response. In the criteria developed by the Japanese Diabetes Society, the diabetic pattern is defined as the fasting blood glucose being higher than 126 mg/dL or the blood glucose level at 120 min being higher than 200 mg/dL. The normal pattern is defined as a fasting blood glucose less than 110 mg/dL and a blood glucose level of less than 140 mg/dL at 120 min.

his wishes, GH treatment was conducted for 6 yr beginning at age 11 despite normal GH secretion. Nevertheless, his final height was 142.4 cm (–4.9 SD).

Thinning of the extremities, due to subcutaneous fat loss, and a moon-face appearance were noticed when the patient was 13 yr old. A whole body CT scan taken at age 19 revealed fatty changes in the liver and an abnormal pattern of subcutaneous fat distribution (Fig. 1c). Dyslipidemia and hyperinsulinism were also evident.

Table 3 Summary of the metabolic profile of the 5 patients

Patient	Fatty liver		Lipid					Adipokines		Diabetes				
	US/CT	ALT (IU/L)	TC (mg/dL)	LDL-C (mg/dL)	TG (mg/dL)	HDL-C (mg/dL)	Treatment	Leptin* (ng/mL)	Adiponectin# (μg/mL)	BG response in OGTT (age)	Insulinogenic index	HOMA-R	HbA1c	Treatment
1	+	56	322	168	675	39	none	18.7	1.6	DM pattern (17 y)	4.63	13.3	6.1%	none
2	+	102	375	203	965	50	none	9.5	6.8	normal (18 y)	1.06	2.92	5.4%	none
3	+	85	284	179	901	44	fenofibrate	10.7	8.5	normal (13 y)	1.04	2.11	5.3%	none
										normal (23 y)	1.47	1.98	5.1%	
4	+	137	314	176	1,073	44	none	17.9	1.7	DM pattern (19 y)	2.34	17.0	5.7%	none
5	+	250	203	124	402	35	none	11.9	3.8	normal (21 y)	3.89	3.15	5.2%	none

+, present; US, ultrasound; CT, computed tomography; ALT, alanine aminotransferase; TC, total cholesterol; LDL-C, LDL-cholesterol; TG, triglyceride; HDL-C, HDL-cholesterol; HOMA-R, homeostasis model assessment ratio; BG, blood glucose; DM, diabetes mellitus; ND, not determined. Each value is the highest one ever determined, except for HDL-C where the lowest value is presented. *Leptin levels in healthy Japanese adolescents were reported to be 1.65 ± 0.78 ng/mL in males and 6.03 ± 3.69 ng/mL in females (35). #Adiponectin levels in healthy young Japanese women were reported to be 6.2–10.0 μg/mL (36). In addition, adiponectin level lower than 6.65 μg/mL was suggested as a diagnostic marker of metabolic syndrome in Japanese children (37).

Patient 4, male, neuroblastoma

A 1-yr-old boy developed exophthalmos and neuroblastoma, originating from the left adrenal, with multiple bone and marrow metastases (stage IV_A). Following total resection of the primary lesion, complete remission was obtained by chemotherapy and radiation (whole skull, 23.4 Gy; right orbit, 18 Gy). Eight months after diagnosis, peripheral blood stemcell transplantation (PBSCT) was carried out, with conditioning that included 12 Gy TBI.

Since age 4, the patient has been receiving L-thyroxine because of primary hypothyroidism (TSH, 22.0 μIU/mL; free T4, 0.78 ng/dL). At age 14, an evaluation for growth failure revealed severe atrophy of the pituitary gland. At that time, abdominal US demonstrated fatty changes in his liver. After a diagnosis of complete GH deficiency, GH treatment was started. At age 18, testosterone administration was introduced due to primary hypogonadism (LH, 7.6 IU/L; FSH, 26.6 IU/L; testosterone, 51 ng/dL).

At 19 yr of age, abnormal liver function tests, dyslipidemia and a moon-face appearance prompted a metabolic reevaluation. Although the degree of aberrant fat distribution was modest compared with other patients, a CT scan demonstrated increased visceral fat with a markedly fatty liver. A diabetic pattern of blood glucose response was observed in an OGTT, as well as pronounced hyperinsulinism.

Patient 5, female, neuroblastoma

A neuroblastoma, with multiple bone metastases (stage IV_A), was diagnosed in a 1-yr-old female during the evaluation of an abdominal mass. Following total removal of the primary tumor and chemotherapy, two consecutive autologous BMTs, without TBI, were performed 3-mo apart. A regional relapse in the right iliac bone, as well as marrow relapse, was found one year later. The patient was treated with an allogeneic BMT, the donor being her 2-locus mismatched sister, following 12 Gy TBI conditioning. Thereafter, complete remission was obtained, and immunosuppressants were withdrawn at age 8.

Partial GH deficiency was diagnosed at age 12, and GH treatment was conducted for 5 yr. The patient also exhibited primary hypogonadism, high-frequency deafness and the presence of cataracts. At around age 17, fatty